Transactions of the Materials Research Society of Japan 29 [3] 835-838 (2004)

Effect of Molecular Structure on the Formation of Chiral Smectic C Phase in Some Ester Compounds

Takeyasu Tasaka, Kazuhide Ota, Koji Kabu, Yuki Morita, Hiroaki Okamoto, and Shunsuke Takenaka

Department of Materials Science and Engineering, Faculty of Engineering, Yamaguchi University,
Tokiwadai 2557, Ube, Yamaguchi 755-8611, Japan
Fax: 81-836-85-9640, e-mail: takenaka@po.cc.yamaguchi-u.ac.jp

This paper describes physicochemical properties of some homologues of (S)-4-(3,7-dimethyloctyloxy)phenyl 4-(3-alkoxy-4-cyanobenzoyloxy)benzoates and 4-alkoxyphenyl (S)-4-[4-cyano-3-3,7-dimethyloctyloxybenzoyloxy]benzoates. These compounds tend to exhibit a chiral smectic C phase. The layer structure was examined by an X-ray diffraction method, and the molecular arrangement in the smectic phase is discussed in terms of the molecular shape.
Key words: liquid crystals, chiral smectic C phase, X-ray, molecular structure, bent shape

1. INTRODUCTION

Linearity, rigidity, and polarizability of molecule are known to be important factors in determining the liquid crystal (LC) properties. Among them, the geometrical factors are a special interest, because these frequently result not only in diversity of phase transition behavior but also molecular arrangement in LC phases. One of the typical examples is some compounds having a notable bent shape within the LC core. The "bent" molecules are also known to exhibit interesting phase transition behavior involving the chiral properties, even if molecules themselves do not involve any chiral factor.[1,2]

A similar "bent" shape would be also expected in conventional calamitic LC materials by introducing a bulky or a long substituent at the lateral position. Therefore, we designed and prepared some derivatives of 4-alkoxyphenyl 4-(3-alkoxy-4-cyanobenzoyloxy)benzoates. For the compounds, the long hydrocarbon chain at the 3-position would extend toward the lateral position of the LC core due to a repulsive interaction between the hydrocarbon chain and the adjacent cyano group, resulting in a "bent" shape of the entire molecule. In our work an (S)-3,7-dimethyloctyl (3,7-DMO) group is selected as one of the long alkoxy groups in connection with the chiral properties of the bent molecules.[2] In this paper, we describe the physicochemical properties of compounds **1** and **2**, and the results will be discussed in terms of the molecular arrangement within the smectic layer.

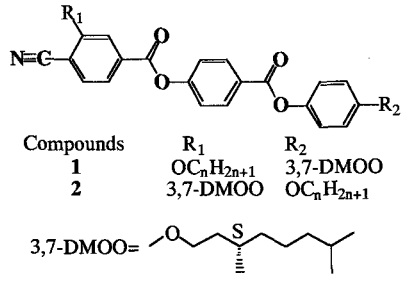

Fig. 1. Molecular structure of compounds **1** and **2**.

2. EXPERIMENTAL

Preparation and method were described in our earlier paper.[3] The molecular orbital parameters were obtained by a semi-empirical molecular orbital method, MOPAC2000, where minimization of the total energy was achieved by an AM1 method.

3. RESULTS

(S)-4-(3,7-dimethyloctyloxy)phenyl-4-(4-cyanobenzoyloxy)-benzoate (**3**), a parent compound of **1** and **2**, has a mesomorphic sequence of

C•99(•SmC*•92)•SmA2•160•SmAd•196•Ch•201•I (T/°C)

In the polymesomorphism C, SmC*, SmA, Ch, and I indicate crystal, chiral smectic C, smectic A, cholesteric, and isotropic phases, respectively. The phase transition temperatures were determined by a microscopic observation, and the latent heats for melting, SmC*-SmA2, SmA2-SmAd, SmAd-Ch, and Ch-I were 13.3, 0.0, 0.0, 0.1, and 0.2 kJ/mol, respectively.

The X-ray profile of **3** showed two reflection maxima at ca. $2\theta = 3°$ as an intense and sharp peak and ca. 20 ° as a weak and broad one. The layer spacing was determined from the former peak, and is plotted against temperature in Fig. 2.

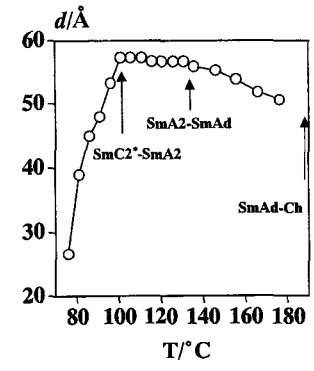

Fig. 2. Temperature dependence of the layer spacing for **3**.

The diffraction peak shows a complex temperature dependency in both SmC* and SmA phases. The layer spacing in the SmAd phase increases with reducing temperature, and gives a maximum of 57.3 Å at ca. 100 °C in the SmA2 phase. The layer spacing corresponds to 1.9 times of the calculated molecular length (28.9 Å). Then, the layer spacing steeply decreases with reducing temperature in the SmC* phase region, and becomes 26.6 Å at 76 °C, just before recrystallization. These results indicate that molecules in the SmA phase form the bilayer (SmA2) and partially bilayer (SmAd) arrangements and in the SmC* one the bilayer (SmC2*) and monolayer (SmC1*) ones. The steep reduction of the layer spacing below 90 °C probably arises from the molecular rearrangement from the bilayer structure to monolayer one.

By introducing the substituent at the 3-position, the phase transition behavior becomes a very simple. Transition temperatures for **1** and **2** are summarized in Tables I and II.

For compounds **1** the homologues with a short hydrocarbon chain (n=4~6) at the 3-position exhibit the SmA phase with a fan texture, and the SmC* phase commences from the hexyloxy homologue, and the SmC*-I transition temperature for the higher homologues almost stays constant at ca. 100 °C. The latent heats for the SmC*-I transition were in the range between 5 and 8 kJ/mol. For compounds **2** the homologues (n=4 and 5) exhibit the Ch phase with a focal conic or a streaked texture, and the SmC* phase is also exhibited below the Ch phase. The SmC*-I (Ch) transition temperature is almost independent of the hydrocarbon chain length. The phase transition behavior of both compounds is similar each other, except the lower homologues.

Table I. Transition temperatures of **1**.

	Transition temperatures (°C)						
n	C		SmC*		SmA		I
4	•	95	-		(•	94)	•
5	•	94	-		(•	93)	•
6	•	95	•	99	•	99	•
7	•	97	•	101	•		•
8	•	96	•	103	•		•
10	•	87	•	104	•		•
12	•	92	•	105	•		•
13	•	90	•	105	•		•
14	•	88	•	104	•		•

C, SmC*, SmA, Ch, and I indicate crystal, chiral smectic C, smectic A, cholesteric and isotropic phases, respectively. Parenthesis indicates a monotropic transition.

Table II. Transition temperatures of **2**.

	Transition temperatures (°C)						
n	C		SmC*		Ch		I
4	•	103	(•	87	•	97)	•
5	•	89	•	92	•	96	•
6	•	87	•	99	•		•
7	•	85	•	100	•		•
8	•	87	•	102	•		•
9	•	85	•	104	•		•
10	•	90	•	105	•		•
12	•	92	•	105	•		•
13	•	93	•	105	•		•
14	•	96	•	105	•		•

Captions refer to footnote in Table I.

For the comparative study, the binary phase diagram for the mixture of **1** and **3** was examined, and the results are shown in Fig. 3.

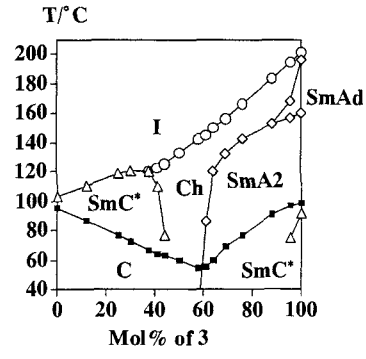

Fig. 3. Binary phase diagram for the mixture of **1** (n= 8, on left) and **3** (on right). Phase transitions below melting point were observed on the cooling process.

The SmAd and SmC* phases are observed only in the range between 88 and 100 mol% of **3**. TheSmA2-Ch transition temperature steeply decreases in the range between 60 and 65 mol% of **3**, and similarly, the SmC*-Ch transition temperature of **1** steeply decreases in the range between 38 and 45 mol% of **3**. As a result, the mixture of 45- 60 mol% of **3** shows a wide range Ch phase. The discontinuous feature in the Sm phases suggests that the mesomorphic properties of **1** and **3** are fairly different each other, especially in the Sm phases. Consequently, the SmC* phases of **1** and **3** have different physical properties.

The X-ray profile in the SmC* phase shows two main reflection maxima at ca. 2θ=3 ° as a sharp and intense peak and ca. 2θ=20 ° as a broad and weak one. The layer spacing in the SmC* phase was calculated from the former peak.

The layer spacings for **1** are plotted against temperature in Fig. 4, and the average layer spacings are plotted against the hydrocarbon number in Fig. 5. The layer spacing in the SmC* phase shown in Fig. 4 is almost independent of temperature, and the entire feature is contrast to **3** in Fig. 2. The layer spacing for the homologues (n=4~8) is almost independent of the hydrocarbon chain length, and interestingly, the layer spacing of ca. 29 Å agrees with the molecular length.

The layer spacings for **2** are plotted against temperature in Fig. 6, and the average layer spacings are plotted against the hydrocarbon number in Fig. 7.

In Fig. 6 the layer spacings are almost independent of temperature, though the plots for some homologues show

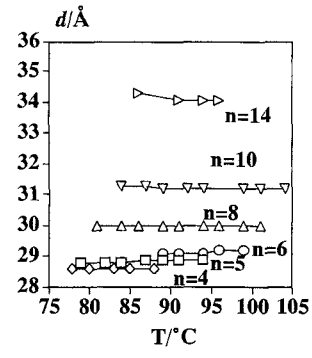

Fig. 4. Plots of layer spacings vs. temperature for **1**. n is the carbon number of the hydrocarbon chain.

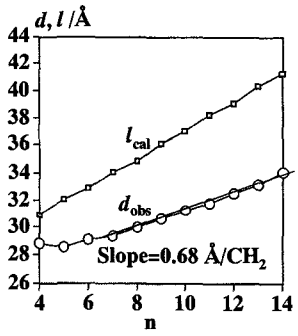

Fig. 5. Plots of layer spacing (d_{obs}, ○) and molecular length (l_{cal}, □) vs. n (carbon number) for **1**. The molecular length (l_{cal}) for the most stable conformation was estimated by a semi-empirical molecular orbital calculation (MOPAC2000). l_{cal} was defined for the conformer in Fig.8

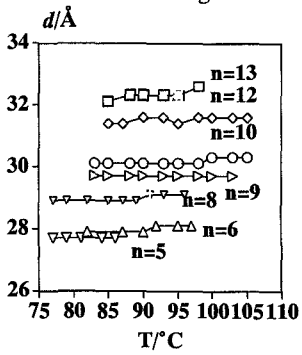

Fig. 6 Plots of layer spacings vs. temperature for **2**.

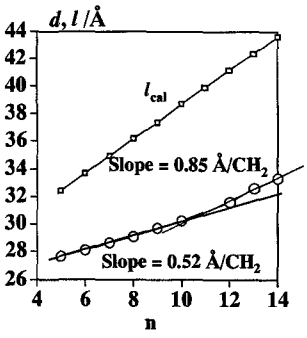

Fig. 7. Plots of layer spacing (d_{obs}) and molecular length (l_{cal}) vs. n for **2**. l_{cal} was defined for the conformer in Fig. 8.

experimental uneven. In Fig. 7 the layer spacings for the lower members (n=5~8) gradually increase with increasing the hydrocarbon chain length, and for the higher ones (>8) tend to increase more rapidly.

4. DISCUSSION

4-Alkoxyphenyl 4-(4-cyanobenzoyloxy)benzoates, the parent compound of **1** and **2**, is one of typical polar LC materials, so that the homologues are expected to exhibit a complex mesomorphism, and **3** is one of the typical cases. The polar interaction of the terminal cyano group should play some important role for the phenomena.[4] However, the complex phase transition behavior disappears in **1** and **2** having the lateral substituent, and the homologues reveal only SmC* phase, and in addition the temperature dependency of the layer spacing is quite small. These results indicate that the hydrocarbon chain substituted at the 3-position weakens the inter-molecular polar interaction around the cyano group, so that the molecules essentially have a monolayer arrangement in the SmC* phase. Therefore, the molecular structure of **1** and **2** was estimated by a semi-empirical molecular orbital calculation (MOPAC2000), where minimization of the total energy was achieved by an AM1 method, and the results are illustrated in Fig. 8.

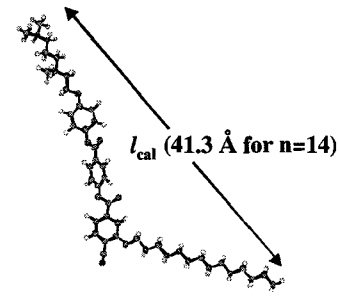

Fig. 8. Molecular structure of the tetradecyloxy homologue of **1**.

The MO calculation suggests that the steric hindrance between the cyano group and the adjacent hydrocarbon chain is so large that the hydrocarbon chain extends toward the opposite site of the cyano group, and extension of the hydrocarbon chain results in the notable bent shape. The longitudinal length, l_{cal}, was calculated from the conformer, and is plotted in Figs. 5 and 7. The calculated molecular length increases with increasing n, where the slope is 1.25 Å/CH$_2$. On the other hand, the observed layer spacings (d_{obs}) of both compounds are notably shorter than the l_{cal} values, and the slopes are fairly small compared with those for l_{cal}. A remarkable fact is that the layer spacings for **1** (n=4~8) in Fig. 5 are almost independent of the hydrocarbon chain length and agree with the calculated longitudinal length of **3** (29.2 Å), indicating that the

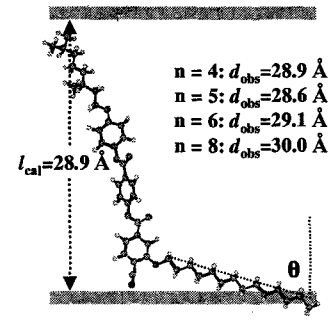

Fig. 9. A possible molecular arrangement in SmC* phase for **1** (n=4~8). The top and bottom lines indicate the layer surface of the SmC* phase.

hydrocarbon chain at the 3-position arranges almost parallel to the SmC* layer plane. A possible molecular arrangement is illustrated in Fig. 9. From the figure, the tilt angle of the hydrocarbon chain at the 3-position (θ) to the surface of the SmC* phase is assumed to be more than 80 °.

Next, we consider the physical meaning of the d_{obs}-n plot and the slope in Figs. 5 and 7 with a simple model shown in Fig. 10. The C-C-C angle and C-C length used in the MO calculation are 111.6 ° and 1.514 Å, respectively. We suppose here that the long hydrocarbon chain always extends linearly with a zigzag conformation in LC states such as N, SmA, and SmC

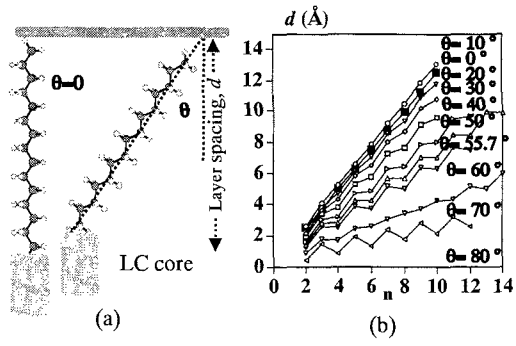

Fig. 10. Relationship between layer spacing (d/Å) and tilt angle (θ) of hydrocarbon chain to the Sm layer. The tilt angle, θ, is the angle between the average line of the hydrocarbon chain and the perpendicular axis of the smectic layer indicated by the heavy lines in (a). In practice, the terminal of the hydrocarbon chain is connected with LC core.

phases. When the average axis of the hydrocarbon chain arranges perpendicular to the smectic layer, the model structure can be illustrated as shown in Fig. 10(a). In such conditions, the layer spacing will increase 1.25 Å/CH_2. If the average axis has a tilt angle, θ, to the smectic layer, d should be given as a function of the hydrocarbon chain number (n) and tilt angle (θ):

for even members

$$d = 0.755n\{\sin(55.65-\theta)+\sin(55.65+\theta)\}$$

for odd members

$$d = 0.755\{(n-1)\sin(55.65-\theta)+(n+1)\sin(55.65+\theta)\}$$

The calculated d values are plotted against the hydrocarbon number in Fig. 10(b). We have to be in mind that θ in the equations is not the conventional tilt angle of the LC molecule in the SmC phase, but that of the hydrocarbon chain to the Sm layer. Three important facts can be drawn from the figure. First, the layer spacing increases 1.25 Å/CH_2, when the average angle of the hydrocarbon chain to the Sm layer is 90 °. The plot for the SmA phase of 4-(4-alkoxyphenoxycarbonyl)phenyl 4-trifluoromethylbenzoates is the case.[5] Second, the linear correlation between the layer spacing and the hydrocarbon number should be lost, if the hydrocarbon chain twists or shrinks. The distortion of the straight line may occur, if the long hydrocarbon chain causes of displacement of the LC core within the Sm phase. The plots of **1** and **2** in Figs. 5 and 7 may correspond to this case. Third, the layer spacing in the Sm phase is expected to show an even-odd alternation in the wide range of θ, and the tendency should be notable, when the tilt angle is near 55 °.[6] We have reported that the layer spacing for the SmC phase of 4-(4-alkoxyphenoxycarbonyl)phenyl 4-octyloxybenzoates shows a remarkable even-odd alternation.[7]

The plot of the layer spacing for **1** (n=8~14) in Fig. 5 can be approximated to a straight line, and gives a slope of 0.68 Å/CH_2. Putting 0.68 to Fig. 10(b) gives the tilt angle of 58 °. That is, the hydrocarbon chain for the higher homologues has an angle of 58 ° to the SmC* layer. It is assumed that for the higher homologues the tilt angle of the LC core is smaller than that of the model in Fig. 9.

The Plot of the layer spacing for **2** in Fig. 7 may be roughly divided into two regions. First, the lower homologues (n=5~9) give a slope of 0.52 Å/CH_2 which corresponds to the tilt angle of 65 °. Second, the slope of 0.85 Å/CH_2 is obtained from the plot for the higher homologues (n=12~14) and corresponds to the tilt angle of 47 °.

The distortion of the straight line should suggest that the molecular arrangement within the SmC* layer gradually varies by changing the hydrocarbon chain length in the present system.

Considering these facts, the calculated molecular models of **2** with n=14 and n=8 are put in the SmC* layer, where the observed layer spacings are 33.3 and 29.1 Å, respectively, and the arrangement models are illustrated in Fig. 11.

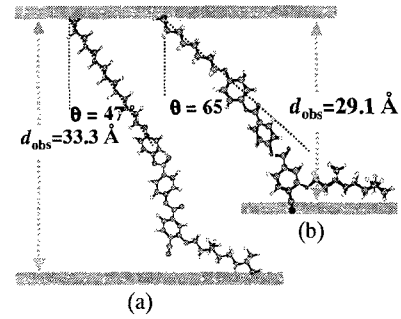

Fig. 11. Possible molecular arrangements in SmC* phase for **2**: (a) n=14, (b) n=8.

As shown in the figure, the calculated molecule is put very good in the observed layer spacing. Similar to the hydrocarbon chain of **1** in Fig. 9, the DMO group attached at the 3-position arranges near the surface of the SmC* layer. On the other hand, the hydrocarbon chain at the opposite position has an angle of 65 ° to the SmC* layer when the hydrocarbon chain is short (n=5~9), and the tilt angle gradually becomes small with increasing n. Of course, the change of the tilt angle should be continuous through the homologous series.

Conclusively, **3** is polar LC, and shows a complex phase transition behavior, where the LC core is assumed to arrange almost perpendicular to the SmA layer. On the other hand, **1** and **2** having a long hydrocarbon chain at the 3-position are the bent molecule, and the tilt arrangement of the LC core due to the packing effect of the lateral long hydrocarbon chain is responsible for the notable evolution of the SmC* phase. Even in compounds **1** and **2**, however, the polar interactions around the cyano group should play some important roles for enhancing LC properties.

We want to emphasize that the present analytical method is a convenient and important tool for the determination of the tilt angle of the hydrocarbon chain to the Sm layer.

References

[1] Y. Matsunaga and S. Miyamoto, *Mol. Cryst. Liq. Cryst.*, **237**, 311 (1993).
[2] D. R. Link, F. Natale, R. Shao, J. E. Maclenman, N. A. Clark, E. Koblova, and D. M. Walba, *Science*, **278**, 1924 (1997).
[3] S. Takenaka, K. Ota, Y. Morita, and H. Okamoto, *Ferroelectrics*, **276**, 73 (2002).
[4] G. W. Gray and J. W. Goodby, 1984, "*Smectic Liquid Crystals*," p.134, Heyden and Son Inc., Philadelphia.
[5] T. Tasaka, H. Okamoto, Y. Morita, K. Kasatani, and S. Takenaka, *Chem. Lett.*, 2002, 536.
[6] M. Duan, H. Okamoto, V. F. Petrov, and S. Takenaka, *Liquid Crystals*, **26** (5), 737 (1999).
[7] T. Tasaka, H. Okamoto, V. F. Petrov, and S. Takenaka, *Liquid Crystals*, **28**, 1025 (2001).

(Received October 14, 2003; Accepted March 12, 2004)